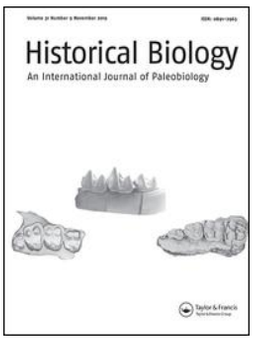

Taylor & Francis
Taylor & Francis Group

Historical Biology
An International Journal of Paleobiology

ISSN: (Print) (Online) Journal homepage: https://www.tandfonline.com/loi/ghbi20

# Temporal variation in soricid dentition: which are first – qualitative or quantitative features?

Leonid L. Voyta, Valeriya E. Omelko, Mikhail P. Tiunov, Ekaterina A. Petrova & Lyudmila Yu. Kryuchkova

**To cite this article:** Leonid L. Voyta, Valeriya E. Omelko, Mikhail P. Tiunov, Ekaterina A. Petrova & Lyudmila Yu. Kryuchkova (2021): Temporal variation in soricid dentition: which are first – qualitative or quantitative features?, Historical Biology, DOI: 10.1080/08912963.2021.1986040

**To link to this article:** https://doi.org/10.1080/08912963.2021.1986040

Published online: 16 Oct 2021.

HISTORICAL BIOLOGY
https://doi.org/10.1080/08912963.2021.1986040

Taylor & Francis
Taylor & Francis Group



# Temporal variation in soricid dentition: which are first – qualitative or quantitative features?

Leonid L. Voyta[a], Valeriya E. Omelko[b], Mikhail P. Tiunov[b], Ekaterina A. Petrova[a] and Lyudmila Yu. Kryuchkova[c]

[a]Laboratory of Theriology, Zoological Institute, Russian Academy of Sciences, Saint Petersburg, Russia; [b]Federal Scientific Center of the East Asia Terrestrial Biodiversity,Far Eastern Branch of Russian Academy of Sciences, Vladivostok, Russia; [c]Saint Petersburg State University, Saint Petersburg, Russia

**ABSTRACT**

The current paper offers a protocol for the analytic assessment of the intraspecific variability of dental morphology in shrews. Our approach blends a temporal aspect together with a comparative morphological analysis in terms of a unified morphogenetic concept based on the 'activator-inhibitor cascades model' and 'decreasing heritability model'. We used material from the upper Pleistocene and Holocene fossiliferous deposits of Koridornaya and Sukhaya caves in the Russian Far East and analysed the first upper molars of specimens that were similar in size to the teeth of *Crocidura lasiura* but differed in some proportions and qualitative features. We analysed the temporal variation of the molar shape against samples of the extant species *C. lasiura, Crocidura sibirica and Crocidura shantungensis* along with fossil specimens using geometric morphometry based on three-dimensional landmarks and semi-landmark datasets. Our results revealed correspondence of the fossil teeth to intraspecies variation of *C. lasiura* with a slight increase in the morphospace size. We also found two deviant teeth, which, however, also fell in the range of *C. lasiura* and were determined as *Crocidura* cf. *C. lasiura*. A detailed description of the dental features became possible with the use of the computed microtomography approach.

**ARTICLE HISTORY**
Received 28 August 2021
Accepted 23 September 2021

**KEYWORDS**
Soricidae; *Crocidura*; Late Pleistocene; temporal variability; East Asia

## Introduction

Shrews (Mammalia, Soricidae) are a taxonomically diverse group of mammals with a broad range of morphological disparities. The extant Soricidae is comprised of 26 genera (Hutterer 2005a; Burgin and He 2018), while fossil taxa are at least twice as diverse, with approximately 60 extinct genera (McKenna and Bell 1997; Reumer 1998; Lopatin 2006a). Since fossil taxa are predominantly represented by teeth, their study is still the most important approach to the investigation of extinct shrews. In the last two decades were developed the modern approaches based on computed microtomography and two- and three-dimensional morphometries allowed the successful analysis of morphological features in different mammalian groups (Wu and Schepartz 2009; Ni et al. 2012; Anemone et al. 2012; Ekdale and Racicot 2015; Mason 2016; Orliac and Billet 2016; Ameen et al. 2017; Cucchi et al. 2017; Almécija et al. 2019; among others). These approaches can be implemented in the shrew fossil teeth analysis and discovery of new features.

### *Shrew dentition and morphogenesis*

The shrew's dentition consists of four types of teeth that are recognised for stem 'insectivorous-level' mammalian groups and divided by position in the rows into incisors, canines, premolars and molars (Ungar 2010). The distal incisors, canines and mesial premolars are similar in crown shape and cannot be easily distinguished; these teeth are thus generally referred to using the terms 'unicuspid' or 'antemolar' (Dannelid 1998). Some modern authors attempted to homologise the shrew's antemolars to incisors, canines and premolars based on anatomy (Hutterer 2005b) and morphological diversity in fossil materials (Lopatin 2006a). However, the authors' conclusions on the dental formula composition and the steps of antemolar reduction are still questionable without information on tooth morphogenesis (e.g. Yamanaka et al. 2007, 2010; Järvinen et al. 2008). The most complex dentition consists of molariform teeth consisting of the fourth upper premolar and three upper and lower molars (P4, M1/m1–M3/m3). These teeth are characterised by dimensional and structural heterogeneities within the tooth row from the first to third molars. Most likely, this heterogeneity is inherent to most eutherian mammals and is clearly described by the sequential inhibitory cascade model (Järvinen et al. 2006; Kavanagh et al. 2007; Renvoisé et al. 2009, 2017; Ahn et al. 2010; Yamanaka and Uemura 2010; Polly and Mock 2017), which explains developmental mechanisms that may guide evolutionary change through 'the activator-inhibitor logic of sequential tooth development' (Kavanagh et al. 2007, p. 427). The model clarifies the differences in the size and complexity of molars within the tooth row. Kavanagh et al. (2007) postulated the activator-inhibitor cascades as adaptive in the dimensional and structural heterogeneities of the teeth between taxa. On the other hand, the shrew's dentition is unique due to the reduction of deciduous teeth (Yamanaka et al. 2007, 2010; Järvinen et al. 2008) and early activation of the first molar development long before animal birth (M1 germ on the 'bud stage' form on the 18th embryonic day in *Suncus murinus* by Yamanaka et al. 2010; a newborn *S. murinus* appears on the 30th embryonic day by Kauffman et al. 2010). In developing the idea of applying the cascade model to the adaptivity of dentition differences, we can suppose that teeth that erupted up to animal birth are minimally affected by the external environment. This thesis was discussed by Polly and Wójcik (2019, p. 344), who wrote for the first

**CONTACT** Leonid L. Voyta leonid.voyta@zin.ru Laboratory of Theriology, Zoological Institute, Russian Academy of Sciences, Universitetskaya Nab. 1, Saint Petersburg 199034, Russia



Published online 16 Oct 2021

lower molar of *Sorex araneus* that 'all non-genetic environmental effects in teeth are buffered both by the individual's own homoeostasis and the homogenous environment of the mother's womb, whereas skeletal traits are not, implying that tooth traits should have higher heritability than skeletal traits and less non-genetic correlation with the animal's microenvironment'. This statement seems clear enough in terms of the significance of the first molar investigation for the determination of the soricid intergroup (phylogenetic) relationships in the fossil material through a modern approach to 'assess the phylogenetic signal in morphological traits' in the sense of Adams (2014) and Polly and Mock (2017).

### Temporal variation of morphological features and its estimation

Estimating the range of temporal variation in morphological features is an important component of palaeotheriology because it directly affects the description of the extinct taxonomic diversity. The significant approach to fossil data actualisation is an analysis of modern organisms. In most cases, the matching of modern and fossil datasets is reduced to size change assessments, where changes have often been interpreted as a response to paleoclimate in accordance with ecological rules (e.g. Bergman rule; see review in Dayan et al. 1993) and, to a lesser extent, interactions between species (e.g. Dayan et al. 1993). However, we can find several articles where authors described the variation in the qualitative features but no significant size changes. The most substantial example of the soricid dentition variation was Reumer's description of two morphotypes of the first molar's hypocone in extinct *Asoriculus gibberodon* (Soricinae; Reumer 1984, p. 94, 99), where morphotype A represented M1 with separate hypocone (material from Hungarian Osztramos 7 site, MN 16; and Csarnóta 2 site, MN 16) and morphotype B with lingually shifted hypocone and associated with the entocingulum (Osztramos 7). Some examples of tooth morphotypes can also be found in Mészáros (1997) and Furió and Agustí (2017). All authors regarded the morphotypes as an intergroup variation. However, the question remains of how to sort intergroup and intragroup differences in fossil data. The answer seems to depend on the palaeontologist's own attitude towards variability. However, there must be a way to assess this analytically.

Reumer (1984) described other changes in M1 of *A. gibberodon* linked to hypocone expressions, such as metaloph absence, narrow separation between the protocone and hypocone and weak posterior emargination. These characteristics and their states are connected with the molar talon, namely, the hypoconal flange (shelf), which is an evolutionary novelty of mammalian dentition (Hunter and Jernvall 1995; Jernvall 1995). As mentioned above, the latest evolutionary tooth parts (hypoconal flange) and separate structures (hypocone) are the first targets of activator-inhibitor cascades during morphogenesis in the sense of Kavanagh et al. (2007). In sum, therefore, the general proportion of molar transformations occurs together with structural changes in the qualitative features, and both quantitative and qualitative changes can be linked to adaptive evolution of the particular shrew lineage. The proportion of the teeth should be understood as a sum of shape and size (Rasskin-Gutman 2003), which can be analysed using geometric morphometric approaches (Claude 2008; Klingenberg 2011; Adams and Otárola-Castillo 2013; Adams 2014; Cornette et al. 2013, 2015; among others), and the qualitative dental features can be precisely analysed using computed microtomography techniques (Anemone et al. 2012).

### Model species selection

The successful study of temporal variation in morphological traits is dependent on the correct selection of the model group. Highly specialised groups, such as Neogene Anourosoricini, cannot be analysed because of the absence of modern analogues for the genera and species that occurred in the Neogene. It is likely that other Neogene groups are unsuitable for this type of analysis for the same reason. However, late Pleistocene species (in this case, Pleistocene shrews) are a better model group because many of the taxa from this time period have survived to the present (see Rzebik-Kowalska 1998; Storch et al. 1998), thus enabling a full description of both past and present variability.

In the current paper, we offer *Crocidura lasiura* as such a model species from the Late Pleistocene and Holocene deposits of the Russian Far East. This species was a good fit for the temporal variation analysis for several reasons: (i) the species has a relatively narrow spatial distribution (Cassola 2016). The Russian part of the geographical range of the analysed samples occupies the northernmost area that provides (ii) the reduced taxonomic diversity of *Crocidura*. The modern *Crocidura* species' Far Eastern assemblage consists of *C. lasiura* and *Crocidura shantungensis* (Zaitsev et al. 2014). Both species are clearly distinguished by size, which provides (iii) unambiguous species determination in both recent and fossil materials. These factors allow us to prepare the simplest protocol for a correct description of the shape changes of the M1 affected by mostly temporal influences (conventionally) without geographic influences.

The main reason we chose to study this particular fossil material of *C. lasiura* was detecting a wide variation of the qualitative features of the M1 crown, such as the presence/absence of the metaloph, different shape and expression of the hypocone and different expression of the posterior emargination. These variations resemble Reumer's features with two morphotypes of M1 of *Asoriculus gibberodon* (Reumer 1984; and see above); however, we could not perceive two or more morphotypes due to the character states' mosaic expression. Therefore, in the current paper, we attempt to estimate the temporal variation of the M1 shape and the structural changes of the tooth crown of *C. lasiura* using three-dimensional approaches of geometric morphometry and computed microtomography. The preliminary hypothesis supposes the possibility of analytic means for an analysis of Reumer's tooth transformation in both quantitative and qualitative directions in the sense of the sequential inhibitory cascade model (Kavanagh et al. 2007; and see above).

## Material and methods

### Sampling

A total of 120 M1 teeth (Appendices A and B) from three species in the genus *Crocidura* were studied. Among them: 22 teeth of *C. lasiura* (eight fossils and six extant specimens), Crocidura *sibirica* (n = 4) and *C. shantungensis* (n = 4) were used for the three-dimensional analysis of the shape variation (Appendix A); 102 teeth of *C. lasiura* were analysed to reveal the variation of the M1 crown qualitative features (hypocone expression, metaloph presence, etc.) using a Wild stereo microscope (Appendix B). The fossil specimens from Koridornaya Cave (our specimens FSC RPRV-KorC-110-11, /111-12, /112-13 and FSC RPRV-KorC-124-25) and Sukhaya Cave (four specimens FSC RPRV-SukC-33-43, /34-44, /35-45 and FSC RPRV-SukC-37-47) are held as part of the fossil collection at the Federal Scientific Centre of the East Asia Terrestrial Biodiversity Far Eastern Branch of the Russian Academy of Sciences (Vladivostok, Russia). Other specimens are

housed in the collections of the Zoological Institute of the Russian Academy of Sciences (St Petersburg, Russia) and the Zoological Museum of Moscow State University (Moscow, Russia); see Appendices A and B for further details. See abbreviated specimen numbers in the table of Appendix C.

### Geometric morphometrics

The first upper molar shape of *Crocidura* was described using a configuration of seven true three-dimensional landmarks (lms) together with 130 three-dimensional semi-landmarks (Figure 1). Both landmark types were prepared using MorphoDig ver. 1.6.0 software (Lebrun 2020). One hundred and thirty semi-landmarks were treated in two steps due to the limitation of the MorphoDig on the export maximal 99 landmarks in the tool 'Export curve segments as landmark file': the first semi-landmark chain runs along the anterior part of the basal tooth contour, from the most anterobuccal point of the metastyllar tooth's corner (8th lm) to a midpoint of the protocone base (47th lm); the second chain runs from a midpoint of the protocone base (47th = 48th lms) around the tooth base contour to the metastyllar corner (8th = 137th lms). Thus, we describe a full basal contour that is clearly defined by a more or less developed ridge. This ridge appears to represent the edge of the enamel layer of the tooth crown, which folds over to the apical side and forms a prominent line. We can define this ridge (line) on both recent and fossil teeth in all analysed species of *Crocidura*. The true landmarks were located on the main styles and cusps of the crown: parastyle (1st lm), paracone (2nd lm), mesostyle (3rd lm), metacone (4th lm), metastyle (5th lm), protocone (6th lm) and hypocone (7th lm). The Procrustes superimposition procedure and principal component analysis (PCA; 'relative warp analyses') were performed with morphologika2 (O'Higgins and Jones 1998). The three-dimensional models of each tooth were obtained based on the computed microtomography data and usage of Avizo 2019.1 software (FEI SAS). For details, see below.

### Shape changes visualisation

Visualisation of the M1 shape transformations revealed by PCA was performed using the statistical and graphic environment R. Based on the main purpose of this paper to describe the temporal variation in the molar shape of specimens from the upper Pleistocene and Holocene deposits of Koridornaya and Sukhaya caves, a single specimen of *Crocidura lasiura* (ZIN 76021) was used as a reference object for the visualisation procedure. This selection was based on the assumption that all fossil specimens were associated with *C. lasiura*. The visualisation script was based on 10 functions of the 'Morpho' and 'Rgl' packages: (i) 'file2mesh' for importing 3D surface files in PLY format (Morpho Package v. 2.8; Schlager 2020, p. 45); (ii) 'read.table' for reading landmark data from VER file (R-Utils; Claude 2008, p. 32); (iii) 'centsiz' for scaling of the targets' landmark datasets (Claude 2008, p. 140); (iv) 'trans1′ for translating each landmark's configuration to the same origin position (Claude 2008, p. 149); (v) 'ild2′ for matching two target landmark configurations after scaling and translating for further superimposition procedures (Claude 2008, p. 155); (vi) 'pPsup' for superimposition of two target landmark configurations (Claude 2008, p. 155); (vii) 'tps3d' for transforming landmark sets via superimposition based on a reference and a target configuration (Morpho Package v. 2.8; Schlager 2020, p. 149); (viii) 'mesh3d: shade3d' for generated 3D objects from imported PLY files (RGL Package v. 0.100.54; Adler and Murdoch 2021, p. 51); (ix) 'plot3d' for plotting 3D objects (RGL

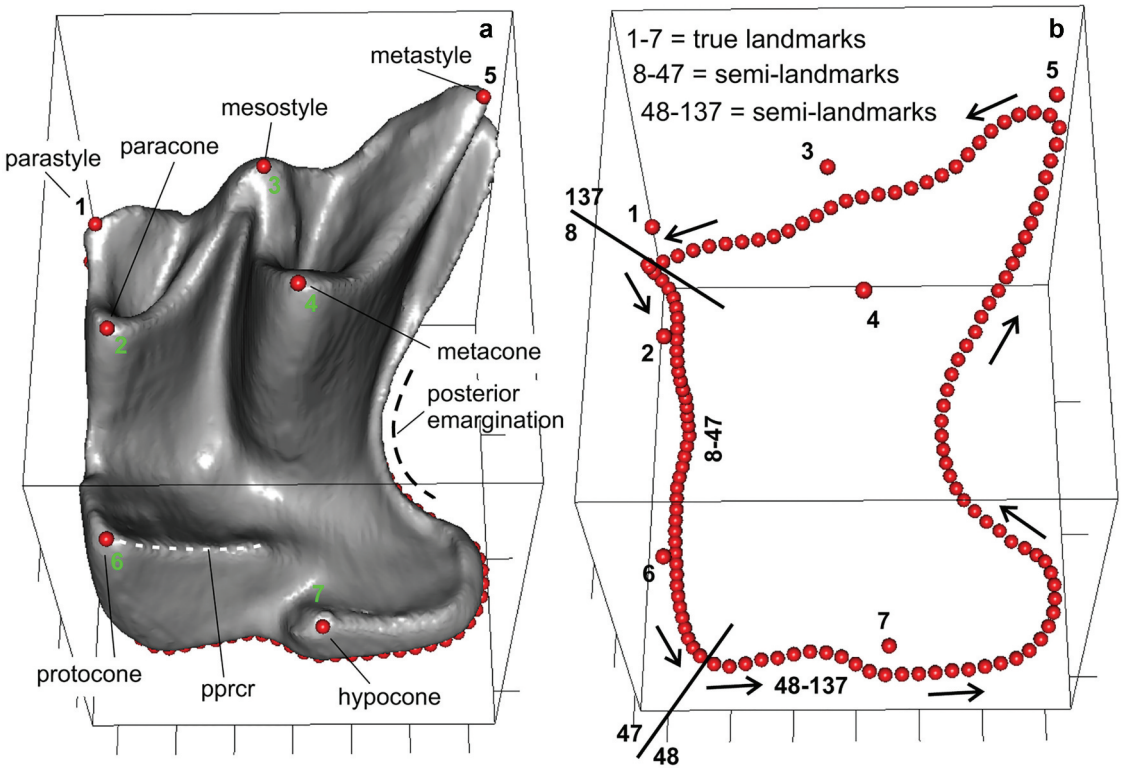


**Figure 1.** Configuration of 7 true landmarks (1–7 lms) and 130 semi-landmarks (8–47 and 48–137 lms) used for analyses of the shape variation of the first upper molar. (a) Three-dimensional model of the first upper left molar of *C. lasiura*. (b) Diagrammatic image explaining the positions of landmarks and semi-landmarks on the enamel surface (styles and cusps) and around the basal contour of the tooth. The arrows mark the direction of the semi-landmark processing. Abbreviations: pprcr – postprotocrista (term by Lopatin 2006b: S212).

Package v. 0.100.54; Adler and Murdoch 2021, p. 82); and (x) 'rgl. snapshot' for saving the screenshot as a PNG file (RGL Package v. 0.100.54; Adler and Murdoch 2021, p. 115). All mesh (PLY) and landmark (VER) files listed in Appendix A are available via request to the corresponding author.

### High-resolution X-ray computed micro-tomography

All analysed shrew specimens were scanned on a SkyScan 1172 Scanner at the Resource Centre for X-ray Diffraction Studies of Saint Petersburg State University (Saint Petersburg, Russia). The SkyScan settings are listed in Appendix A. All specimens were scanned in three-slice mode. Preliminary processing was performed with DataViewer ver. 1.5.4.0 (SkyScan, Brucker). The main processing of the tooth structure (three-dimensional digital reconstruction, surface rendering and measurements) was performed using Avizo 2019.1 (FEI SAS). For all scanned specimens, three-dimensional models (surfaces) of the whole M1 were prepared. The qualitative characteristics expression of M1, such as the presence of metaloph and hypocone, was analysed using three separate three-dimensional models: (i) model of the enamel-dentine junction (EDJ); (ii) model of the outer enamel surface (EOS); and (iii) model of the pulp endocast (see below 'New terms' section). The analysis was carried out according to the methodology of Anemone et al. (2012) and Voyta et al. (2020a).

### Variability

We used two directions of variability testing to minimise metering error effects on the results. The first is the age-related variation of the true landmark positions on the tips of the cusps and styles. The second is the repeatability of the semi-landmark chains around the basal contour of the tooth. In both cases, we used repeated landmark and semi-landmark placement three times via 3 to 5 hours of skip to minimise metering error. The analysis was performed on the mean values of these replicates. The addition means of the error test is a visual assessment of the position of the specimens within the principal component space (morphospace). For this test, we added samples of *C. shantungensis* (sympatric and coexistent with *C. lasiura*) and *C. sibirica* (geographically 'nearest' to *C. lasiura* northernmost *Crocidura* species). We assumed that if the metering error would be high, then the species samples would be mixed. The satisfactory error will correspond to the clear hiatus between all species. The presence of both immature and mature specimens in all species samples makes the visual test even more meaningful, as well as the presence of males and females. In addition, to avoid age-related variation, we corrected the positions of the true landmark when a landmark on a cusp appeared shifted due to wear; the supposed 'unworn position' was indicated by the condition of the immature specimen. The correctness of this approach was tested visually by the final PCA.

### Geological settings for C. lasiura from Russian Far East

The analysed material represents maxilla fragments with upper molariform teeth in different combinations (single M1, M1 with P4 and/or M2). These materials originate from deposits of two limestone caves, Koridornaya and Sukhaya. The caves' fossiliferous samples are being processed for sorting of the remains of the different taxonomic groups; therefore, the first upper molars (Appendix C) analysed in this paper (n = 8) are a small part of the remaining mass unsorted material. Both places were included in the modern limits of the distribution range of *C. lasiura* (Cassola 2016).

The limestone Koridornaya Cave is located in the southeastern spurs of the Lesser Khingan Ridge, the southern part of the Pompeevskii Ridge and the right bank of the Stolbukha River (approximately N 48°00′, E 130°59′; Jewish Autonomous Oblast, Far East, Russia) and is described in Voyta et al. (2020b). Sediments were selected during excavation with a conditional horizon (layers) of 10 cm. *C. lasiura*-like (same-sized) fragments were found in the layers 50–60 cm (three specimens KRD-011, KRD-012, KRD-013) and 100–110 cm (specimen FSC RPRV- KRD-025). In this locality from the 60–70 cm layer, redeposited remains of the extant soricine shrew *Beremendia minor* (Soricidae) were described (Voyta et al. 2020b). A roe deer metacarpal bone from the 110–120 cm layer was 14 C-dated by the AMS method to ~50,000 yr BP (Voyta et al. 2020b).

The limestone Sukhaya Cave is located 3–5 km from Barabash village in the northwestern part of the Manchurian-Korean Mountains (approximately N 43°09′, E 131°28′; Khasansky District of Primorsky Krai; Far East, Russia) and is described by Kosintsev et al. (2020), Tiunov and Gimranov (2020) and Tiunov and Gusev (2021). *C. lasiura*-like (same-sized) fragments were found in the layers 20–30 cm (three specimens SKH-043, SKH-044, SKH-045) and 30–40 cm (specimen SKH-047). In this locality from the 30–40 cm, 50–60 cm and 60–70 cm layers, a new species of the genus *Petaurista* (Rodentia: Sciuridae) was described by Tiunov and Gimranov (2020); and one new ochotonid genius, *Tonomochotona*, with three new species by Tiunov and Gusev (2021). Two horse tooth fragments (*Equus* sp.) were isolated from the layers 30–40 cm (sample Eq-Suh/2: UCSC ID SC17. AV073) and 50–60 cm (sample Eq-Suh/5: UCSC ID SC17.AV075). Both fragments were 14 C-dated by the AMS method to ~50,000 yr BP (Tiunov and Gimranov 2020).

According to the 14 C AMS dates (see Tiunov and Gimranov 2020; Voyta et al. 2020b), the mammalian species association and the degree of preservation of fossil remains, all the layers above a depth of 120 cm are considered Holocene and Late Pleistocene with lower limits earlier than 130 yr BP. For the purposes of this paper, we conventionally assume that the materials from the 100–110 cm layer of Koridornaya Cave and from the 20–30 and 30–40 layers of Sukhaya Cave originate from the Late Pleistocene (~50–46 yr BP), and other materials from the deposits above 60 cm depth of Koridornaya Cave originate from the Holocene time span.

### New terms and acronyms

(1) 'Decreasing heritability model' or 'Polly-Mock model' by Polly and Mock (2017), the model describes the extent of the phylogenetic signal (heritability index, $h^2$) within the shrew's (tribosphenic) molar crown elements; (2) 'pulp endocast surface' (PES), an outer surface of the three-dimensional model of the tooth pulp. Used for the analysis and sequential description of the crown elements expression from the outer enamel surface (OES) through the surface of the enamel-dentine junction (EDJ) to PES (by Anemone et al. 2012; Voyta et al. 2020a).

## Results

### Variation of the upper molar crown and root features

The first upper molar of *C. lasiura* is strongly compressed in the anteroposterior direction, which is a typical characteristic of Crocidurinae. Visually, M1 has an oblique buccal margin, and in this proportion, it is clearly different from M2. The ectoloph ('centrocrista' by Lopatin 2006b), which is composed of the postparacrista and premetacrista, is strongly folded. The trigone basin is

deep and narrow. The postprotocrista ends straight without a noticeable bulge; the metaloph is absent. The hypoconal flange is moderately shifted posteriorly and, therefore, the posterior emargination is well developed; the hypocone is usually well defined and connects with the anterior part of the hypoconal flange ridge. The area between the postprotocrista and hypocone is a slightly concave valley without any ridges. These crown characteristics occur in most first upper molars of *C. lasiura* as well as in other species, such as *C. shantungensis* and *C. sibirica* (Figure 2) used in the present work for comparisons. The review of *C. lasiura* specimens from the zoological collections (Appendix B) and fossil material (Appendix C) revealed 79% of the teeth with typical crown features (the remaining 21% have deviant features). The apical (radicular) part of the *C. lasiura* tooth is also similar to other crocidurines and bears five roots: the antero- and posterobuccal roots, the anterolingual root (ALR), the additional anterolingual root, which is placed under the protocone lobe together with ALR, and the hypoconal flange root (Figure 2: A4–A5). The endodontic characteristics on the enamel-dentine junction (EDJ) and in the pulpal chambers and canals (pulp endocast surface, PES) quite strictly correspond to the structures on the outer enamel surface (OES; Figure 2A). All ridges, cusps and styles are reflected in the EDJ and PES. Some age-related parts in the central area of PES are overgrown during maturation (Figure 2A3 cf. C) while maintaining the functional passability of the canals and the volume of the chambers as previously described for soricines (see details in Voyta et al. 2020a).

The fossil teeth from the Koridornaya and Sukhaya caves display deviant structures such as (i) the presence of the metaloph (Figure 2B) or the bulged end of the postprotocrista with bending towards the metacone base (Appendix C: KRD-011–013, SKH-045); (ii) the cone-like hypocone separated from the hypoconal flange ridge (Figure 2B; Appendix C: KRD-011, SKH-043); and (iii) the hypocone with additional ridges (Appendix C: SKH-047). The endodontic characters allow for the determination of characters on OES: the metaloph clearly defined on EDJ (Figure 2B); the hypocone and the anterior end of the hypoconal flange ridge are separated, however, the PES displays the connection of the canal with the hypoconal chamber in the usual contrition (Figure 2: B3 cf. A3 and C). In addition, we can see different degrees of posterior expansion of the hypoconal flange and, therefore, the depth of the posterior emargination (Appendix C: KRD-025 cf. KRD-012). Surprisingly, in the recent samples, we also found deviant features, which are similar to those described for the fossil materials (the metaloph presence; Appendix B) and the following additional features: (iv) the end of the postprotocrista is bent towards the hypocone and (v) the hypocone unexpressed, the crest of the hypoconal flange bent to the postprotocrista end (Appendix B). The fossil specimens, except KRD-025, have five separated roots, as described for other crocidurines. Specimen KRD-025 has four roots; however, the PES allows the determination of two radicular canals, which correspond to the anterolingual root and additional anterobuccal root. In sum, therefore, the specimen has three separate roots and two fused roots (five total). This fusion is similar to the usual character of the other *Crocidura* when the broad and short hypoconal flange root bears two separated radicular canals quite often with two separate apical foramina (unpublished data).

### *First upper molar shape and size variation*

*C. lasiura* differs from *C. shantungensis* and *C. sibirica* in larger overall size. The smallest *C. shantungensis* and medium-sized *C. sibirica* clearly differed by the anterior width of the M1 (Figure 3B) and for any other metric feature. All fossil specimens in our analysis had tooth sizes similar to recent samples of *C. lasiura* (Appendix C).

Principal component analysis revealed clear differences between all species samples based on the three-dimensional landmark and semi-landmark datasets: *C. lasiura* vs. *C. shantungensis* vs. *C. sibirica* (Figure 3A). We described the shape differences depicted in the morphospace defined by the two first components, PC 1 and 2, which together account for 52% of the variation. The most important interspecies shape differences of the M1 revealed along the first component (36.5% of the total variance) were associated with transformations of the tooth base described by the semi-landmarks ('basal contour' differences); the differences in position of the cusps and styles were relatively minor (coronal differences). *C. lasiura* differs from *C. shantungensis* in the deeper posterior emargination, in a straighter lingual tooth outline, in the more buccal position of the parastyle and a more undulated anterior outline that is visible in the anterior view (Figure 3C). The second component (15.5%) described both coronal and basal contour differences and can be well shown between the other two *Crocidura* species. *C. sibirica* differs from *C. shantungensis* in the height of the cusps and styles (1–7 lms), in the buccal shifting of the tips of the paracone, metacone, protocone and hypocone and in the anterior protrusion of the anterior tooth outline (Figure 3D).

Based on the shape differences between the modern species samples, we could try to determine the relative position of the fossil specimens in the morphospace defined by the first two principal components. Six specimens were positioned in the *C. lasiura* morphospace, namely, KRD-011, KRD-013, SKH-043, SKH-044, SKH-047. Two specimens, KRD-012 and KRD-025, were located within the *C. lasiura* range along the first component but at the opposite ends of the second component quite far from the *C. lasiura* sample centroid (around 0 at PC 2). The differences between typical *C. lasiura* (ZIN 76021) and both outlying specimens are shown in Figure 4. The KRD-012 (positive end of the PC 2) differs from *C. lasiura* in the anterolingual protrusion of the parastyle (1st lm and semi-landmarks), in the posterolingual shift of the mesostyle (5th lm and semi-landmarks), in the narrowing and posterior protrusion of the hypoconal flange and in the posterior shift of the anterior tooth outline (Figure 4A). In the overall proportion, KRD-012 is narrower, with a protruding narrow hypoconal flange and a shorter metastyllar lobe (Figure 4B), than recent specimens of *C. lasiura*. KRD-025 (negative end of PC 2) differs from *C. lasiura* in the extreme anteroposterior compression of the tooth crown with the short hypoconal flange and very shallow posterior emargination (Figure 4: C–D).

## Discussion

### *General remarks*

By comparing extinct groups from various points in time with related extant taxa, palaeontologists can distinguish between intergroup and intragroup variations. However, even an experienced palaeontologist can be faced with unexpected character variations, as stated by Simpson (1970, p. 2) in the introduction to his description of Argyrolagidae (Metatheria). Because of this, we need to search for a new approach to analytically assess the limits of intragroup variation. In the past, traditional palaeotheriology used both qualitative and quantitative means for assessments, which cannot always provide an unambiguous answer to the question – is it a new form or intraspecies form? In addition, the situation is complicated by the absence of

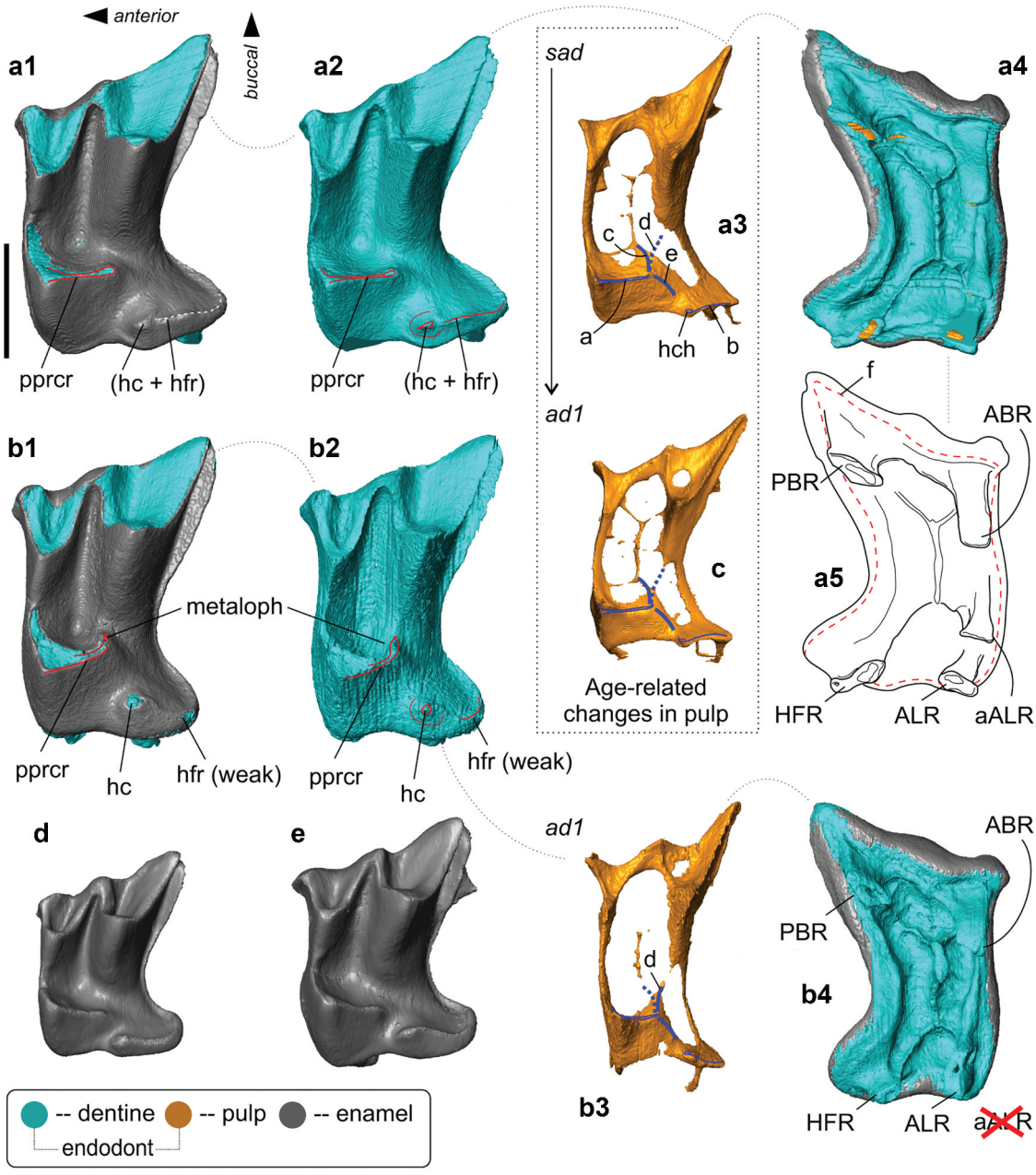


**Figure 2.** Three-dimensional models of the first upper molars, enamel-dentine junction (EDJ) surfaces and pulpal endocasts of *Crocidura* species: (A1–4) *C. lasiura*, ZIN 76015; (B1–4) *Crocidura* cf. *lasiura*, FSC RPRV-KorC-124-25 (mirror view); (C) *C. lasiura*, ZIN 89335; (D) *C. shantungensis*, ZIN 89469; (E) *C. sibirica*, ZIN 79423. (A1, B1) The models (EOS + EDJ) of left M1 in occlusal view with combined enamel and dentine surfaces; (A2, B2) The models of EDJ of left M1 in occlusal view. (A3, B3, C) The models of PES of left M1 in occlusal view. (A4, B4) The models (EOS + EDJ) of left M1 in apical view. (D, E) The models of left M1 in occlusal view without separation of the enamel and dentine. (A5) Explanatory drawing of the tooth apical surface. Abbreviations: a – pulpal expression of the postprotocrista (pprcr); aALR – additional anterolingual root; ABR – anterobiccal root (by Voyta et al. 2020a); ad1 – mature specimen (detail see in Voyta et al. 2020a); ALR – anterolingual root; b – pulpal protrusion of the hypoconal flange ridge (hfr); c – pulpal protrusion of the preliminary connection between the pprcr end and the base of paracone (solid line – linked in immature animals; dotted line – the canal overgrown); d – pulpal protrusion (bridge) of the preliminary connection between the pprcr end and the base of metacone, i.e. the metaloph base; e – pulpal protrusion of the preliminary connection between the pprcr end and the hypocone; f – border of the enamel layer on the apical surface of the tooth; dotted red line marks the contour for the semi-landmarks location; hc – hypocone; hch – hypocone pulp chamber; HFR – hypoconal flange root; PBR – posterobuccal root; sad – immature specimen. All teeth in the same scale. Scale bar is 1 mm.

a clear theoretical basis for describing morphological variability. For instance, there is a problem of homologisation of the shrew upper antemolars that has been solved by modern researchers in different ways based on empirical data (see introduction section; Hutterer 2005b; Lopatin 2006a). This problem is, in turn, a part of a larger issue in the dental formula evolution of Soricidae. The necessary theoretical basis for the homology of antemolar teeth is provided by works on the morphogenesis of shrew teeth with the timing of deciduous and permanent tooth development (Yamanaka et al. 2007, 2010; Järvinen et al. 2008). The sequential inhibitory cascade model (Järvinen et al. 2006; Kavanagh et al. 2007) is a theoretical basis for the explanation of tooth expression differences during foetal morphogenesis, which correspond to phenotypic differences between taxa in antemolar numbers. Nevertheless, this theoretical base has not yet been applied to explain empirical observations.

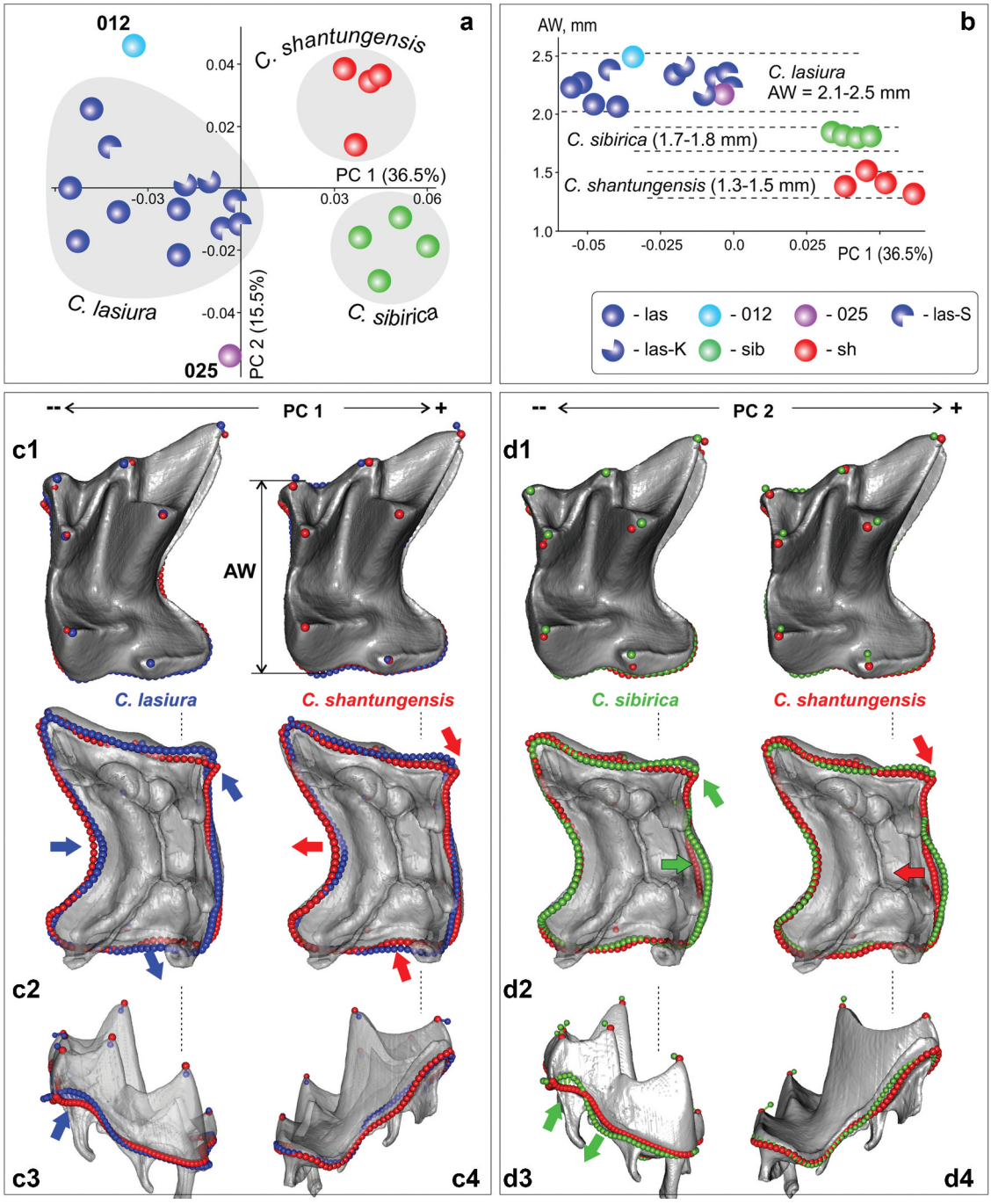


**Figure 3.** Results of the first upper molar shape analysis of the samples of *C. lasiura, C. shantungensis* and *C. sibirica* based on three-dimensional landmark and semi-landmark dataset. (a) Principal component plot for three samples of the recent species and eight fossil specimens from Koridornaya and Sukhaya caves (first vs. second components). (b) Bivariate plot with information on the size (anterior width, AW, vertical axis) and the shape (PC 1, horizontal axis) for three species and eight fossil specimens. (C1) The occlusal views of the visualised shape transformations between *C. lasiura* (left, blue lms) and *C. shantungensis* (right, red lms) corresponding to differences along PC 1. (C2) The apical views . . . (*ibid*.). (C3) The anterior view of the shape transformation of *C. lasiura*. (C4) The posterior view of the shape transformation of *C. shantungensis*. (D1) The occlusal views of the visualised shape transformations between *C. sibirica* (left, green lms) and *C. shantungensis* (right, red lms) corresponding to differences along PC 2. (D2) The apical views . . . (*ibid*.). (D3) The anterior view of the shape transformation of *C. sibirica*. (D4) The posterior view of the shape transformation of *C. shantungensis*. Coloured arrows mark differences in pair accordingly the species colour (*C. lasiura*, blue; *C. shantungensis*, red; *C. sibirica*, green). Abbreviations: 012 – fossil specimen KRD-012 (light blue); 025 – fossil specimen KRD-025 (fuchsine); las – six recent specimens of *C. lasiura*; las-K – two fossil specimens from Koridornaya Cave; las-S – four fossil specimens from Sukhaya Cave; sib – four recent specimens of *C. sibirica*; sh – four recent specimens of *C. shantungensis*.

Our work is the first attempt to integrate the theoretical framework on shrew tooth morphogenesis with an analytical method to determine the limits of intragroup variations in the temporal aspect. The analytic method is based on the three-dimensional geometric morphometric approach (O'Higgins and Jones 1998; Claude 2008; Klingenberg 2011; Adams and Otárola-Castillo 2013; Cornette et al. 2013, 2015; Schlager 2017; and others) that allows a precise description and accurate analysis of the shape of complex morphological structures, such as soricid tribosphenic molars. Previous work by Cornette et al. (2015) displayed the high geographic variation in bone plasticity based on the interactions between bones, muscles and bite force in *Crocidura* species populations. According to

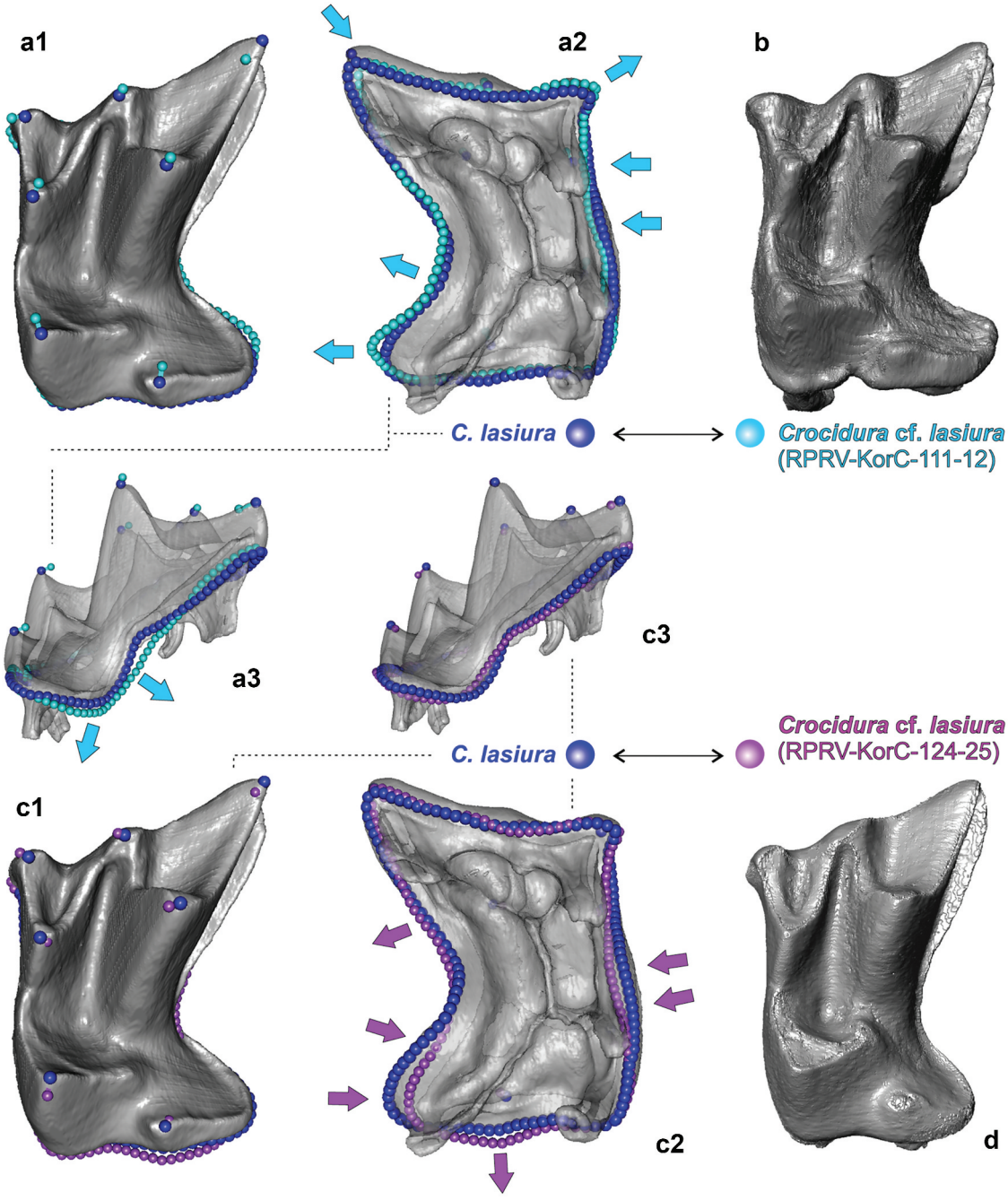


**Figure 4.** The first upper molar shape transformation along PC 2 for two pairs: (A) *C. lasiura* (blue) and fossil specimen KRD-012 (light blue); (C) *C. lasiura* (blue) and fossil specimen KRD-025 (fuchsine). (B) Three-dimensional model of M1 of KRD-012 in occlusal (mirror) view. (D) Three-dimensional model of M1 ofKRD-025 in occlusal (mirror) view. (A1, C1) Models of M1 in occlusal view. (A2, C2) *ibid*., in apical view. (A3, C3) *ibid*., in anterior view. Unscaled (the teeth sizes see in Appendix 3).

Young and Badyaev (2010), this plasticity can relate to the maintenance of local adaptations with evolutionary diversification in morphology. These results and conclusions were the basis of our first attempt to examine the analytic assessment of the variation within fossil data. The work of Polly and Wójcik (2019; and earlier by Polly and Mock 2017) raised the issue of participation of the phylogenetic and epigenetic (non-genetic) components in the shape variation of the different shrew morphological structures, such as the skull, hemimandible and first lower molar. Since the first molar (upper and lower) is least susceptible to the influence of the environment during morphogenesis (Polly and Wójcik 2019, p. 344), we proposed the first upper molar as a good morphological structure to determine the limits of the intragroup variations compared to the more generally used cranial and mandibular structures.

### *Temporal variation in the M1 shape and its taxonomic implications*

Perhaps, the most important conclusion from our results is the hierarchy of the phenetic differences between species revealed by the three-dimensional shape analysis approach. The results of the principal component analysis display clear differentiation between three species (*C. lasiura, C. sibirica* and *C. shantungensis*) in the M1

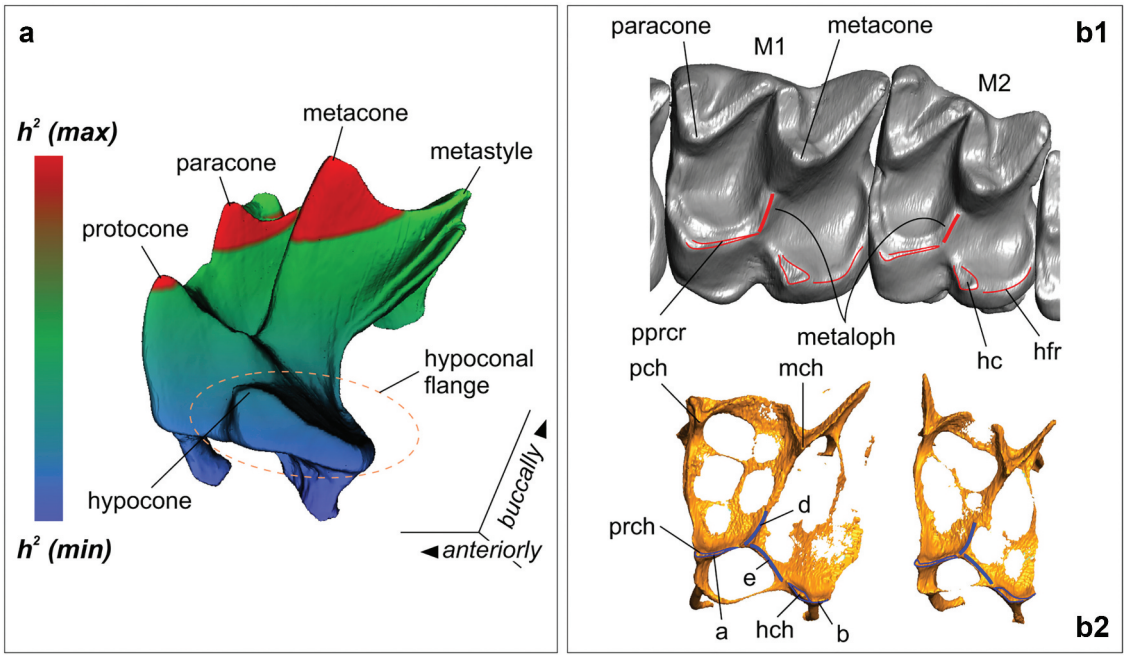


**Figure 5.** Diagrammatic image of the supposed distribution of the 'heritability index' ($h^2$) on the first upper molar from maximal to minimal values in correspondence to the 'decreasing heritability model' by Polly and Mock (2017) (A). The three-dimensional model (unicoloured EOS + EDJ) (B1) and PES (B2) of the upper first and second molars of *Blarina brevicauda* in occlusal views. Abbreviations: mch – metacone pulp chamber; pch – paracone pulp chamber; prch – protocone pulp chamber; also see in figure 2. Unscaled.

shape (Figure 3), when the more significant characteristics varied along the first principal component, and were associated with the basal contour of the tooth (130 semi-landmarks). In contrast to expectations, crown differences, such as variation in cusp position (1–7 lms), varied along the second principal component.

The hierarchy of revealed differences allows for a fresh view of the variation of the qualitative characters. Because the cusp variation within the tooth crown occupied a smaller part of the total variance (PC 2, 15.5%) than the variance of the basal contour, we can conclude, first, high similarity in the crown morphology between all three species based on a moderate variation of the position of the tips of the paracone, metacone and protocone between them and, second, the presence of the loaded characters in the folding of the basal contour. Both aspects of the variability correspond to conclusions by Polly and Mock (2017), who revealed a decreasing heritability index from the tips of the cusps of the first lower molar of *Cryptotis* (Soricinae) to the notches between them. This decrease in the heritability index from the upper part to the lower part of the crown conforms to the model of molar morphogenesis, where the earlier crown structures (i.e., tips of the main cusps; see overview in Polly and Mock 2017) have a higher phylogenetic signal (heritability index, $h^2$) than the later structures (Figure 5A). Actually, the 'evolutionary latest tooth parts', hypoconal flange and hypocone, mentioned in the introduction, as the first target of the activator-inhibitor cascades during morphogenesis, should be considered as a particular case of the Polly and Mock (2017) idea on the different participation of the phylogenetic and epigenetic components in the shape variation of the first molar of Soricidae. In summary, the high degree of variation of the lower part of the crown, including basal contour folding, is an expression of the epigenetic component of morphogenesis, i.e., adaptivity. The geographic and temporal variations of the structures of the lower part of the tooth crown corresponds to the realisation of the different trajectories of the adaptive strategies within the species, which can be revealed in the morphospace broadening (for a review of the morphospace concept, see Voyta et al. 2020b). This thesis is confirmed by the high percentage (approximately 21%) of variation of the qualitative characteristics of the M1 crown, which were shown in most fossil teeth and partly in the modern samples of *C. laisura*. The deviant characteristics were associated with the hypoconal flange (Appendix B).

According to this concept, the limits of temporal variation in the tooth shape between six fossil specimens (Appendix C) correspond to intraspecies variation of *C. lasiura* with a slight increase of the morphospace size. Two specimens from Koridornaya Cave (Figure 4) displayed a deviant tooth shape, which, however, laid within the *C. lasiura* limits along the first principal component (Figure 3A), and in the current paper, they are considered *Crocidura* cf. *C. lasiura* (Appendix C). We could not detect a pronounced dependence between the fossil specimen positions within the principal component space and the differences in the conditional horizons of the cave deposits, except perhaps deviant tooth KRD-025 from the deepest layer (100–110 cm) of Koridornaya Cave.

However, because there were redeposited *Beremendia minor* found in the Koridornaya Cave deposits in the 60–70 cm layer (Voyta et al. 2020b), we have to consider the possible redeposition of the deviant teeth, at least for specimen KRD-025 from the deeper layer of 100–110 cm than the mentioned findings of *B. minor*. We hope to resolve this issue by using more representative tooth material from Koridornaya Cave, including analysis of the first lower molar shape.

### Endodontic features

Endodontic structures, such as enamel dentine junction (EDJ) as an outer part of the dentine and pulpal endocast surface (PES) as an outer part of the pulp, can be reconstructed using micro-CT data to

help describe and analyse different qualitative characteristics on the outer enamel surface (OES). Anemone et al. (2012) proposed a protocol to check the expression of dental crown features using comparisons of both OES and EDJ. In this paper, we develop our idea (Voyta et al. 2020a) on the use of pulpal endocasts for the analysis of dental variability and propose adding to Anemone's protocol. Accordingly, we used reconstruction of EDJ of all fossil specimens and reference specimens (Figure 2A) from extant samples of *C. lasiura* for estimation of the unusual characters in the fossil teeth, namely the metaloph expression and the separation of the hypocone. In all cases, the features on OES repeated on EDJ. PES revealed two different variants: (i) the usual teeth of *C. lasiura* without the metaloph display the early overgrowing of the pulp below the end of postprotocrista (Figure 2: A3 and C, see d); (ii) the retention of the pulpal canal between the posterobuccal part of the protocone chamber and anterolingual part of the metacone chamber as a bottom of the metaloph on EDJ and OES of the deviant teeth (Figure 2B, see d). These two variants help us to determine the morphogenetic base of the metaloph expression because the pulp can form a bridge between the protocone and metacone chambers. In the first variant, the bridge was very weak and did not provide metaloph expression; in the second variant, bridge formation began at an earlier stage and was expressed in the metaloph or metaloph-like bulge. The realisation of both variants conforms to the Polly and Mock (2017) concept and reflects adaptive effects similar to those described for the basal contour of M1. The metaloph is an unusual feature among Crocidurinae; but it may appear in the evolution of the group, as there is a basal structure, which can be found in PES. In this case, the presence of metaloph in some individuals (approximately 10% among analysed specimens of *C. lasiura*) is not surprising. The soricine shrews are more diverse in this feature, and we can find a good example of the earlier development of a metaloph bridge in the PES of *Blarina brevicauda* (Soricinae) on M1 and M2 (Figure 5B).

The development of additional crests around the hypocone (or towards the hypocone) may explain the rare variation in the extant samples of *C. lasiura* (Appendix B: 2.2 and 2.3), which can increase in fossil materials. We detected two additional low crests at the hypocone in M1 from the Sukhaya Cave (Appendix C: SKH-047). EDJ precisely repeated both crests; PES repeated only one crest towards the end of the postprotocrista.

### *Variability*

Age and quite often sex variability affect all mammalian groups and are a ubiquitous problem in morphometric analysis. The tips of the paracone, metacone, protocone and hypocone, as well as the tips of the styles, are strongly influenced by age and can affect the results of the shape analysis. The results of the principal component analysis showed (Figure 3A) the correct selection of the analysed specimens where the sample of *C. shantungensis* consisted of immature animals, the samples of *C. sibirica* and *C. lasiura*, including the fossil specimens, consisted of both immature and mature animals (Appendix A), and correct implementation of the three-time repeating protocol in the landmark and semi-landmark processing. The correctness can be assessed visually on the PCA plot by the broad hiatus between species samples (Figure 3A). In addition, the most significant differences between species were revealed in the folding of the tooth basal contour (130 semi-landmarks), which seemed unrelated to age.

As mentioned in the introduction, the first molar is minimally influenced by the environment during foetal morphogenesis in comparison to cranial and mandibular bones (see Polly and Wójcik 2019). This thesis is based on the particularities of the shrew's dental morphogenesis and suggests no influence of any morphological effects, e.g. 'Dehnel's phenomenon' for *Sorex* (Lázaro and Dechmann 2021) or sexual dimorphism for *Crocidura* (Zidarova 2015), which can arise after tooth mineralisation (Polly and Wójcik 2019, p. 344). In sum, therefore, we can neglect sexual dimorphism in the first molar shape analysis.

## Conclusions

### *Which are first – qualitative or quantitative features*

The current paper offers a protocol for the analytical assessment of intraspecific variability in the upper molar shape. We combine a temporal aspect with a qualitative dental analysis in terms of a unified theoretical morphogenetic concept based on the 'activator-inhibitor cascades model' by Kavanagh et al. (2007) and 'decreasing heritability model' by Polly and Mock (2017). Our development of a new protocol set based on a three-dimensional geometric morphometric approach, principal component analysis, computed microtomography data and obtained results allows us to meaningfully answer the following question: which comes first in intraspecific variability assessment – qualitative or quantitative features? The qualitative characteristics are exceedingly variable and display a high rate of homoplasy. For instance, the cladistic analysis of African Crocidurinae by McLellan (1994) based on morphological traits revealed a low rate of consistency index (CI = 0.25) and a correspondingly high rate of homoplasy. We also know that several morphological features repeatedly converged in different shrew lineages, a pattern that became clear after the widespread use of molecular methods (e.g. see position of Asian and African *Suncus* in Dubey et al. (2008) and Upham et al. (2019)). In this case, molecular phylogenies can provide correct analysis (correct navigation) of the qualitative morphological characters in extant groups considering intergroup relationships. However, since molecular methods most often cannot be employed for palaeontological material, correct navigation in the analysis of qualitative characters can be provided by morphometric analysis. As we demonstrate in the current study, geometric morphometric analysis based on modern theory has a broad potential to describe the temporal aspect of morphological variability. Advanced analysis with our protocols will provide a description of both temporal and spatial aspects by building the required wireframe of inter- and intragroup relationships. In summary, the analysis of the quantitative features based on the modern methods of geometric morphometrics is the first in the intergroup and intragroup variability assessment. Proper quantitative analysis allows a correct qualitative feature analysis.

### *Prospects of protocol use*

Integrative analysis of the quantitative and qualitative features of the first upper molar shape using geometric morphometry and computed microtomography has both methodological and factological prospects. Methodologically, we need to know the resolving power of our protocols in the use of the first upper molar for the analysis of variability on a wider scale than we implemented here. In the current paper, we deliberately limited the morphospace size by using narrowly distributed *Crocidura* species in the morphometric analysis to avoid simultaneous descriptions of both spatial and temporal factors. Future studies should cover both factors by expanding the analysis to include widely distributed species, such as *Crocidura suaveolens* for the northern Palaearctic or other species depending on the geographic region and taxonomic

group. Another aspect is a comparison of the results based on the three-dimensional shape analyses of upper and lower molars (e.g. M1/m1 and other molariform teeth). This comparison may be justified by the unknown upper dentition in some extinct taxa (e.g. some genera of Crocidosoricinae). The imposition of the results can be advanced by estimating phylogenetic signal expression (Klingenberg and Gidaszewski 2010; Adams and Otárola-Castillo 2013). There are several important unresolved issues where our protocols can help. For instance, at present, an extinct ancestor of the modern subfamily Crocidurinae is still unknown. The oldest undetermined Crocidurinae findings have been reported from two middle-Miocene localities and one late-Miocene locality in Turkey (Engesser 1980; Storch et al. 1998). Another undetermined Crocidurinae from a Spanish middle-Miocene locality (Sesé 1980) was re-evaluated as a new genus of Crocidosoricinae, *Turiasorex* (Van Dam et al. 2011). Several early supposedly crocidurines were described from Pakistan and Indian localities (see overview in Flynn et al. 2020). Butler (1998) also noted Middle Miocene findings of the crocidosoricine *Lartetium* (see also Hugueney et al. 2015) and some early findings of the modern genus *Myosorex* in Africa, but neither genus has recently been associated with true crocidurines (Hutterer 2005a; Furió et al. 2007; Hugueney et al. 2015). Other later Pliocene and Pleistocene records have belonged to the modern crocidurine genera (Butler and Greenwood 1979; Butler et al. 1989; Butler 1998; Storch et al. 1998; Furió et al. 2007; Mészáros et al. 2020). Molecular data have helped determine the approximate time of the group split and speculate on the region of origin; however, the ancestral group remains unknown, and exact data on the divergence time are unavailable, except, for example, molecular data on the split between Myosoricinae and Crocidurinae 16.5 Myr ago (Dubey et al. 2007). A new study by Flynn et al. (2020) based on fossil records from the middle and upper Miocene Siwalik deposits in Pakistan described the supposed early appearance of 'cf. *Crocidura* sp'. in Asia approximately 14 Myr ago (middle Miocene). Several specimens from Siwalik deposits of Pakistan, namely, the isolated first lower left molar (YGSP 36182) from the Y733 layer, the isolated second lower left molar (YGSP 36216) from the Y59 layer and the isolated first upper incisor (YGSP 36279) from the Y641 layer date to 14–13 Myr ago. However, at present, these unique materials have not yet been subjected to special morphological analysis to test an ancestor–descendant relationship to the modern genera of Crocidurinae or other groups of Crocidosoricinae. Our protocols set is available for such an analysis.

## Acknowledgments

This study was completed within the framework of the Federal themes of the Zoological Institute no. AAAA-A19-119032590102-7 'Phylogeny, morphology, and systematics of placental mammals'. This study was partly funded by Project no. 19-04-00049 of the Russian Foundation for Fundamental Investigations. The study used the collection materials of the Zoological Institute of the Russian Academy of Sciences (http://www.ckp-rf.ru/usu/73561/), the Zoological Museum of the Moscow State University and the Federal Scientific Centre of the East Asia Terrestrial Biodiversity, FEB RAS.

## Disclosure statement

No potential conflict of interest was reported by the author(s).

## Authors' contributions

LV: a general conception, design, analysis and interpretation of the data and results; drafting the article and preparing of all graphic materials; geometric morphometric analysis; corresponding author.

LV and EP: three-dimensional model preparation by Avizo 2019.1 software (FEI SAS); getting the three-dimensional landmarks and semi-landmarks sets by MorphoDig ver. 1.6.0 software; approval of the final version.

VO and MT: excavation and preliminary preparation of the fossil remains of *Crocidura* from Koridornaya and Sukhaya caves (Russian Far East); revising the manuscript text and images; approval of the final version.

LK: computed microtomography (SkyScan 1172) of the fossil and recent specimens and preliminary preparation of the image stacks of each analysed specimen; approval of the final version.

## Funding

This research was funded in part by the Russian Foundation for Fundamental Investigations [grant number 19-04-00049].

## ORCID

Leonid L. Voyta http://orcid.org/0000-0002-0167-9401
Valeriya E. Omelko http://orcid.org/0000-0002-1285-384X
Mikhail P. Tiunov http://orcid.org/0000-0002-4276-4266
Ekaterina A. Petrova http://orcid.org/0000-0002-7322-8490

## References

Adams DC. 2014. A generalized K statistic for estimating phylogenetic signal from shape and other high-dimensional multivariate data. Syst Biol. 63 (5):685–697. doi:10.1093/sysbio/syu030.

Adams DC, Otárola-Castillo E. 2013. geomorph: an r package for the collection and analysis of geometric morphometric shape data. Methods Ecol Evol. 4 (4):393–399. doi:10.1111/2041-210X.12035.

Adler D, Murdoch D 2021. Package 'rgl', Version 0.104.16. Available at: https://cran.r-project.org/web/packages/rgl/rgl.pdf

Ahn Y, Sanderson BW, Klein OD, Krumlauf R. 2010. Inhibition of Wnt signaling by Wise (Sostdc1) and negative feedback from Shh controls tooth number and patterning. Development. 137(19):3221–3231. doi:10.1242/dev.054668.

Almécija S, Tallman M, Sallam H, Fleagle J, Hammond A, Seiffert E. 2019. Early anthropoid femora reveal divergent adaptive trajectories in catarrhine hind-limb evolution. Nat Commun. 10(1):4778. doi:10.1038/s41467-019-12742-0.

Ameen C, Hulme-Beaman A, Evin A, Genmonpré M, Britton K, Cucchi T, Larson G, Dobney K. 2017. A landmark-based approach for assessing the reliability of mandibular tooth crowding as a marker of dog domestication. J Archaeol Sci. 85:41–50. doi:10.1016/j.jas.2017.06.014.

Anemone RL, Skinner MM, Dirks W. 2012. Are there two distinct types of hypocone in Eocene primates? The 'pseudohypocone' of notharctines revisited. Palaeontol Electronica, 15:15.3.26A.

Burgin CJ, He K 2018. Family Soricidae. In: Wilson DE, Russell AM, editors. Hand book of the mammals of the world. Vol. 8. Insectivores, sloths and colugos. Barcelona: Lynx Edicions; p. 332–551.

Butler PM. 1998. Fossil history of shrews in Africa. In: Wójcik JM, Wolsan M, editors. Evolution of Shrews. Białowieża: mammal Research Institute Polish Academy of Sciences. p. 121–132.

Butler PM, Greenwood M. 1979. Soricidae (Mammalia) from the Early Pleistocene of Olduvai Gorge, Tanzania. Zool J Linnean Soc. 67 (4):329–379. doi:10.1111/j.1096-3642.1979.tb01119.x.

Butler PM, Thorpe RS, Greenwood M. 1989. Interspecific relations of African crocidurine shrews (Mammalia: soricidae) based on multivariate analysis of mandibular date. Zool J Linnean Soc. 96(4):373–412. doi:10.1111/j.1096-3642.1989.tb02520.x.

Cassola F 2016. *Crocidura lasiura* (errata version published in 2017). The IUCN Red List of Threatened Species 2016: e.T41327A115178387.

Claude J. 2008. Morphometrics with R. New York: Springer Science+Business Media, LLC.

Cornette R, Baylac M, Souter T, Herrel A. 2013. Does shape co-variation between the skull and the mandible have functional consequences? A 3D approach for a 3D problem. J Anat. 223(4):329–336. doi:10.1111/joa.12086.

Cornette R, Tresset A, Houssin C, Pascal M, Herrel A. 2015. Does bite force provide a competitive advantage in shrews? The case of the greater white-toothed shrew. Biol J Linn Soc. 114(4):795–807. doi:10.1111/bij.12423.

Cucchi T, Mohaseb A, Peigné S, Debue K, Orlando L, Mashkour M. 2017. Detecting taxonomic and phylogenetic signals in equid cheek teeth: towards new palaeontological and archaeological proxies. R Soc Open Sci. 4 (4):160997. doi:10.1098/rsos.160997.

Dannelid E. 1998. Dental adaptations in shrew. In: Wójcik JM, Wolsan M, editors. Evolution of Shrews. Białowieża: Mammal Research Institute Polish Academy of Sciences; p. 157–174.

Dayan T, Simberloff D, Tchernov E. 1993. Morphological change in Quaternary mammals: a role for species interactions? In: Ra M, Ad B, editors. Morphological change in Quaternary mammals of North America. New York: Cambridge University Press; p. 71–83.

Dubey S, Salamin N, Ohdachi SD, Barrière P, Vogel P. 2007. Molecular phylogenetics of shrews (Mammalia: soricidae) reveal timing of transcontinental colonization. Mol Phylogenet Evol. 44(1):126–137. doi:10.1016/j.ympev.2006.12.002.

Dubey S, Salamin N, Ruedi M, Barrière P, Colyn M, Vogel P. 2008. Biogeographic origin and radiation of the Old World crocidurine shrews (Mammalia: soricidae) inferred from mitochondrial and nuclear genes. Mol Phylogenet Evol. 48(3):953–963. doi:10.1016/j.ympev.2008.07.002.

Ekdale EG, Racicot RA. 2015. Anatomical evidence for low frequency sensitivity in an archaeocete whale: comparison of the inner ear of *Zygorhiza kochii* with that of crown Mysticeti. J Anat. 226(1):22–39. doi:10.1111/joa.12253.

Engesser B. 1980. Insectivora und Chiroptera (Mammalia) aus dem Neogen der Türkei. Schweizerische Paläontologische Abhandlungen. 102:4–149.

Flynn LJ, Jacobs LL, Kimura Y, Taylor LH, Tomida Y. 2020. Siwalik fossil Soricidae: a calibration point for the molecular phylogeny of *Suncus*. Paludicola. 12:247–258.

Furió M, Agustí J. 2017. Latest Miocene insectivores from Eastern Spain: evidence for enhanced latitudinal differences during the Messinian. Geobios. 50(2):123–140. doi:10.1016/j.geobios.2017.02.001.

Furió M, Santos-Cubedo A, Minwer-Barakat R, Agusti J. 2007. Evolutionary history of the African soricid *Myosorex* (Insectivora, Mammalia) out of Africa. J Vertebr Paleontol. 27(4):1018–1032. doi:10.1671/0272-4634(2007)27[1018:EHOTAS]2.0.CO;2.

Hugueney M, Maridet O, Mein P, Mourer-Chauviré C. 2015. *Lartetium africanum* (Lavocat, 1961) (Eulipotyphla · Soricidae) from Beni-Mellal (Morocco), the oldest African shrew: new descriptions, palaeoenvironment and comments on biochronological context. Palaeobiodiversity Palaeoenvironments. 95(3):465–476. doi:10.1007/s12549-015-0197-9.

Hunter JP, Jernvall J. 1995. The hypocone as a key innovation in mammalian evolution. PNAS. 92(23):10718–10722. doi:10.1073/pnas.92.23.10718.

Hutterer R. 2005a. Order Soricomorpha. In: Wilson DE, Reeder DA, editors. Mammal species of the world: a taxonomical reference. 3rd edition ed. Vol. 1. Baltimore: Johns Hopkins University Press; p. 220–311.

Hutterer R. 2005b. Homology of unicuspid and tooth nomenclature in shrews. In: Merritt JF, Churcfield S, Hutterer R, Sheftel BI, editors. Advances in the biology of shrews II. New York: International Society of Shrew Biologists; p. 397–404.

Järvinen E, Salazar-Ciudad I, Birchmeier W, Taketo MM, Jernvall J, Thesleff I. 2006. Continuous tooth generation in mouse is induced by activated epithelial Wnt/β-catenin signaling. PNAS. 103(49):18627–18632. doi:10.1073/pnas.0607289103.

Järvinen E, Välimäki K, Pummila M, Thesleff I, Jernvall J. 2008. The timing of the shrew milk teeth. Evol Dev. 10(4):477–486. doi:10.1111/j.1525-142X.2008.00258.x.

Jernvall J. 1995. Mammalian molar cusp patterns: developmental mechanisms of diversity. Acta Zool Fenn. 198:1–61.

Kauffman AS, Bojkowska K, Rissman EF. 2010. Critical periods of susceptibility to short-term energy challenge during pregnancy: impact on fertility and offspring development. Physiol Behav. 99(1):100–108. doi:10.1016/j.physbeh.2009.10.017.

Kavanagh KD, Evans AR, Jernvall J. 2007. Predicting evolutionary patterns of mammalian teeth from development. Nature. 449(7161):427–432. doi:10.1038/nature06153.

Klingenberg CP. 2011. MorphoJ: an integrated software package for geometric morphometrics. Mol Ecol Resour. 11(2):353–357. doi:10.1111/j.1755-0998.2010.02924.x.

Klingenberg CP, Gidaszewski NA. 2010. Testing and quantifying phylogenetic signals and homoplasy in morphometric data. Syst Biol. 59(3):245–261. doi:10.1093/sysbio/syp106.

Kosintsev PA, Zykov SV, Tiunov MP, Shpansky AV, Gasilin VV, Gimranov DO, Devjashin MM. 2020. The first find of Merck's Rhinoceros (Mammalia, Perissodactyla, Rhinocerotidae, *Stephanorhinus kirchbergensis* Jäger, 1839) remains in the Russian Far East. Doklady Biological Sciences. 491(1):47–49. doi:10.1134/S0012496620010032.

Lázaro J, Dechmann DKN. 2021. Dehnel's phenomenon. Curr Biol. 31(10): R459–R466. doi:10.1016/j.cub.2021.04.006.

Lebrun R 2020. MorphoDig User's guide. Available at: https://morphomuseum.com/tutorialsMorphoDig

Lopatin AV. 2006a. The origin of shrew family (Soricidae, Mammalia): paleontological data. In: Rozhnov SV, editor. Evolution of biosphera and biodiversity. Moscow: KMK Sci. Press; p. 233–245.

Lopatin AV. 2006b. Early Paleogene insectivore mammals of Asia and establishment of the major group of Insectivora. Paleontological Journal. 40:205–405.

Mason MJ. 2016. Structure and function of the mammalian middle ear. I: large middle ears in small desert mammals. J Anat. 228(2):284–299. doi:10.1111/joa.12313.

McKenna MC, Bell SK. 1997. Classification of mammals above the species level. New York: Columbia University Press.

McLellan LJ. 1994. Evolution and phylogenetic affinities of the African species of *Crocidura, Suncus*, and *Sylvisorex* (Insectivora: soricidae). In: Merritt JF, Kirkland GL, Rose RK, editors. Advances in the biology of shrews. Pittsburg: Carnegie Museum of Natural History; p. 379–391.

Mészáros L. 1997. *Kordosia*, a new genus for some late Miocene Amblycoptini shrews (Mammalia, Insectivora). Neues Jahr Geol Palaeontol Monatsh. 2:65–78.

Mészáros L, Botka D, Gasparik M. 2020. Establishing a neotype for *Crocidura obtusa* Kretzoi, 1938 (Mammalia, Soricidae): an emended description of this Pleistocene white-toothed shrew species. PalZ. 94(2):367–375. doi:10.1007/s12542-019-00458-x.

Ni X, Flynn JJ, Wyss AR. 2012. Imaging the inner ear in fossil mammals: high-resolution CT scanning and 3-D virtual reconstruction. Palaeontol Electron. 15.2.18A:1–10.

O'Higgins P, Jones N. 1998. Facial growth in *Cercocebus torquatus*: an application of three-dimensional geometric morphometric techniques to the study of morphological variation. J Anat. 193(2):251–272. doi:10.1046/j.1469-7580.1998.19320251.x.

Orliac MJ, Billet G. 2016. Fallen in a dead ear: intralabyrinthine preservation of stapes in fossil artiodactyls. Palaeovertebrata. 40(1):1–10. doi:10.18563/pv.40.1.e3.

Polly PD, Wójcik JM. 2019. Geometric morphometric tests for phenotypic divergence between chromosomal races. In: Searle JB, Zima J, Polly PD, editors. Shrews, Chromosomes and Speciation. Cambridge: Cambridge University Press; p. 336–364.

Polly PD, Mock OB. 2017. Heritability: the link between development and the microevolution of molar tooth form. Hist Biol. 30(1–2):53–63. doi:10.1080/08912963.2017.1337760.

Rasskin-Gutman D. 2003. Boundary constraints for the emergence of form. In: Müller GB, Callebaut W, editors. Origination of Organismal Form. Massachusetts: MIT Press; p. 305–322.

Renvoisé E, Evans AR, Jebrane A, Labruère C, Laffont R, Montuire S. 2009. Evolution of mammalian tooth patterns: new insights from a developmental prediction model. Evolution. 63(5):1327–1340. doi:10.1111/j.1558-5646.2009.00639.x.

Renvoisé E, Kavanagh KD, Lazzari V, Häkkinen TJ, Rice R, Pantalacci S, Salazar-Ciudad I, Jernvall J. 2017. Mechanical constraint from growing jaw facilitates mammalian dental diversity. PNAS. 114(35):9403–9408. doi:10.1073/pnas.1707410114.

Reumer JWF. 1984. Ruscinian and Early Pleistocene Soricidae (Insectivora, Mammalia) from Tegelen (The Netherlands) and Hungary. Scr Geol. 73:1–173.

Reumer JWF. 1998. A classification of fossil and recent shrews. In: Wójcik JM, Wolsan M, editors. Evolution of Shrews. Białowieża: Mammal Research Institute Polish Academy of Sciences; p. 5–22.

Rzebik-Kowalska B. 1998. Fossil history of shrews in Europe. In: Wójcik JM, Wolsan M, editors. Evolution of Shrews. Białowieża: Mammal Research Institute Polish Academy of Sciences; p. 23–92.

Schlager S. 2017. Morpho and Rvcg – shape Analysis in R: r-packages for geometric morphometrics, shape analysis and surface manipulations. In: Zheng G, Li S, Szekely G, editors. Statistical Shape and Deformation Analysis. 1st. Edition ed. San Diego: Academic Press Inc.; p. 217–256.

Schlager S 2020. Package 'Morpho': calculations and visualisations related to geometric morphometrics. https://cran.r-project.org/web/packages/Morpho/Morpho.pdf. Downloaded on 2021 Aug 26.

Sesé C. 1980. Mamíferos del Miocene Medio de Escobosa de Calatanazor. Madrid: Universidad Complutense de Madrid.

Simpson PP. 1970. The Argyrolagidae, extinct South American marsupials. Bull Mus Comp Zool. 139:1–86.

Storch G, Qiu Z, Zazhigin V. 1998. Fossil history of shrews in Asia. In: Wójcik JM, Wolsan M, editors. Evolution of Shrews. Białowieża: Mammal Research Institute Polish Academy of Sciences; p. 93–120.

Tiunov MP, Gimranov DO. 2020. The first fossil *Petaurista* (Mammalia: Sciuridae) from the Russian Far East and its paleogeographic significance. Palaeoworld. 29(1):176–181. doi:10.1016/j.palwor.2019.05.007.

Tiunov MP, Gusev AE. 2021. A new extinct ochotonid genus from the late Pleistocene of the Russian Far East. Palaeoworld. 30(3):562–572. doi:10.1016/j.palwor.2020.08.003.

Ungar PS. 2010. Mammal teeth: origin, evolution, and diversity. Baltimore (MD): Johns Hopkins University Press.
Upham NS, Esselstyn JA, Jetz W. 2019. Inferring the mammal tree: species-level sets of phylogenies for questions in ecology, evolution, and conservation. PLoS Biol. 17(12):e3000494. doi:10.1371/journal.pbio.3000494.
Van Dam JA, van den Hoek Ostende LW, Reumer JWF. 2011. A new short-snouted shrew from the Miocene of Spain. Geobios. 44(2–3):299–307. doi:10.1016/j.geobios.2010.11.007.
Voyta LL, Omelko VE, Tiunov MP, Vinokurova MV. 2020b. When beremendiin shrews disappeared in East Asia, or how we can estimate fossil redeposition. Hist Biol. Available at:1–12. doi:10.1080/08912963.2020.1822354
Voyta LL, Zazhigin VS, Petrova EA, Krjutchkova L. 2020a. Shrew dentition (Lipotyphla: soricidae) — endodontic morphology and its phylogenetic resolving power. Mammal Res. 65(1):33–48. doi:10.1007/s13364-019-00455-0.
Wu X, Schepartz LA. 2009. Application of computed tomography in paleoanthropological research. Prog Nat Sci. 19(8):913–921. doi:10.1016/j.pnsc.2008.10.009.
Yamanaka A, Sonomura YK, Uemura M. 2007. Development of heterodont dentition in house shrew (*Suncus murinus*). Eur J Oral Sci. 115(6):433–440. doi:10.1111/j.1600-0722.2007.00499.x.
Yamanaka A, Uemura M. 2010. The house shrew, *Suncus murinus*, as a model organism to investigate mammalian basal condition of tooth development. J Oral Biosci. 52(3):215–224. doi:10.1016/S1349-0079(10)80024-6.
Yamanaka A, Yasui K, Sonomura T, Iwai H, Uemura M. 2010. Development of deciduous and permanent dentitions in the upper jaw of the house shrew (*Suncus murinus*). Arch Oral Biol. 55(4):279–287. doi:10.1016/j.archoralbio.2010.02.006.
Young RL, Badyaev AV. 2010. Developmental plasticity links local adaptation and evolutionary diversification in foraging morphology. J Exp Zool B Mol Dev Evol. 314(6):434–444. doi:10.1002/jez.b.21349.
Zaitsev MV, Voyta LL, Sheftel BI 2014. The mammals of Russia and adjacent territories. Lipotyphlans. St. Petersburg: Izdatel'stvo "Nauka." [in Russian]
Zidarova S. 2015. Is there sexual size dimorphism in shrews? A case study of six European species of the family Soricidae. Acta Zool Bulg. 67:19–34.

## Appendix A

List of the specimens analysed by the three-dimensional approach of geometric morphometry with technical information on the computed microtomography scanning. Institutional acronyms: FSC – the Federal Scientific Centre of the East Asia Terrestrial Biodiversity Far Eastern Branch of the Russian Academy of Sciences (Vladivostok, Russia); ZMMU – the Zoological Museum of the Moscow State University (Moscow, Russia); ZIN – the Zoological Institute of the Russian Academy of Sciences (St Petersburg, Russia). Locality acronyms: GVR – Spasskii Disrtrict [Gaivoronskii], Primorsky Krai, Russia (Coll.: Viktor G. Yudin, 1980s); KHS – Khasan Village vicinity, Khasansky District, Primorsky Krai, Russia (Coll.: Maria V. Okhotina, 1970s); KMR – Saltimakovo Village vicinity, Krapivinsky District, Kemerovskaya Oblast', Russia (Coll.: Vladimir E. Sergeev, 1980s); KRD – Koridornaya Cave; SKH – Sukhaya Cave. Age: s – immature specimen (subadult, unworn teeth); ad – mature specimen (adult, slightly or moderate worn teeth). Sex: m – male; f – female. Micro-CT settings given in the following order: acceleration voltage (Kv); resolution (μm); rotation angle (deg.); exposure (ms).

| Collection number | Species (age, sex) | Locality | micro-CT settings |
|---|---|---|---|
| ZIN 76015 | *Crocidura lasiura* (m,s) | GVR | 70/4.41/0.20/1800 |
| ZIN 76017 | *C. lasiura* (m,s) | GVR | 70/4.41/0.20/1800 |
| ZIN 76019 | *C. lasiura* (f,s) | GVR | 80/6.89/0.21/740 |
| ZIN 76020 | *C. lasiura* (f,s) | GVR | 70/4.07/0.25/1700 |
| ZIN 76021 | *C. lasiura* (f,s) | GVR | 70/4.07/0.25/1700 |
| ZIN 89357 | *C. lasiura* (m,s) | KHS | 70/4.48/0.20/1700 |
| FSC RPRV-KorC-110-11 | *C. lasiura* (?,ad) | KRD | 100/2.48/0.20/1550 |
| FSC RPRV-KorC-112-13 | *C. lasiura* (?,ad) | KRD | 100/2.48/0.20/1550 |
| FSC RPRV-SukC-33-43 | *C. lasiura* (?,ad) | SKH | 59/2.28/0.20/1520 |
| FSC RPRV-SukC-34-44 | *C. lasiura* (?,s) | SKH | 59/2.28/0.20/1520 |
| FSC RPRV-SukC-35-45 | *C. lasiura* (?,s) | SKH | 59/2.28/0.20/1520 |
| FSK RPRV-SukC-37-47 | *C. lasiura* (?,ad) | SKH | 59/2.28/0.20/1520 |
| FSC RPRV-KorC-111-12 | *Crocidura* cf. *C. lasiura* (?, ad) | KRD | 100/2.48/0.20/1550 |
| FSC RPRV-KorC-124-25 | *Crocidura* cf. *C. lasiura* (?, ad) | KRD | 89/3.98/0.20/1650 |
| ZIN 89427 | *C. shantungensis* (f,s) | KHS | 74/4.58/0.20/1450 |
| ZIN 89433 | *C. shantungensis* (f,s) | KHS | 74/4.58/0.20/1450 |
| ZIN 89445 | *C. shantungensis* (f,s) | KHS | 74/4.58/0.20/1500 |
| ZIN 89469 | *C. shantungensis* (m,s) | KHS | 74/4.58/0.20/1500 |
| ZIN 79423 | *C. sibirica* (m,ad) | KMR | 74/4.58/0.20/1500 |
| ZIN 79431 | *C. sibirica* (m,s) | KMR | 74/4.58/0.20/1500 |
| ZIN 79437 | *C. sibirica* (f,s) | KMR | 74/4.58/0.20/1450 |
| ZIN 79439 | *C. sibirica* (f,s) | KMR | 74/4.58/0.20/1450 |

**Total**: 22 specimens

## Appendix B

List of the specimens analysed for the assessment of the variation of the qualitative features. For abbreviations, see Appendix A.

**1. Modern samples of *C. lasiura* with the typical features of the first upper molar crown (n = 87)**:

*Amurskaya Oblast'* – **ZMMU** S-201277; S-201278; S-201279.

*Jewish Autonomous Oblast'* – **ZMMU** S-83245; S-83246; S-83247; S-83249; S-83250; S-83251; S-83252; S-83253; S-83254; S-83255.

*Khabarovsky Krai* – **ZMMU** S-74611; S-74612; S-78486; S-195839; S-195840; S-195841.

*Primorsky Krai* – **ZMMU** S-8847; S-8848; S-32575; S-55296; S-55316; S-74675; S-77731; S-77732; S-83156; S-83158; S-83159; S-83160; S-83162; S-83163; S-83164; S-83165; S-83166; S-83228; S-83232; S-83233; S-83234; S-83235; S-83236; S-83237; S-83238; S-83239; S-83240; S-83241; S-83242; S-83243; S-83244; S-83261; S-83266; S-83268; S-83275; S-83277; S-83281; S-83282; S-173212; S-196942; **ZIN** 76008; 76009; 76010; 76011; 76012; 76013; 76016; 76018; 76022; 76799; 76800; 76801; 76803; 76804; 76805; 76806; 76807; 76812; 76813; 76814; 76815; 76817; 76818; 98594; 98598; 103118; 103119; 103120.

**2. Modern samples of *C. lasiura* with deviant features of the first upper molar crown (n = 11)**:

***2.1. Metaloph is present (the postprotocrista end bent towards the metacone base)***:

*Primorsky Krai* – **ZMMU** S-14577; S-14579; S-83161; S-8323; S-83272; S-196941.

***2.2. Postprotocrista end bent to the hypocone***:

*Primorsky Krai* – **ZMMU** S-39443; S-77733; S-173213; S-173214 (and two specimens from FSC collection nos. 11,001, 11,003).

***2.3. Hypocone unexpressed, the crest of the hypoconal flange bent to the postprotocrista end***:

*Primorsky Krai* – **ZIN** 69005.

## Appendix C

(1) Images of the first upper molars of *C. lasiura* and *Crocidura* cf. *C. lasiura* from the Upper Pleistocene and Holocene deposits of Koridornaya Cave (FSC RPRV-KorC-124-25, FSC RPRV-KorC-110-11, /111-12, /112-13) and Sukhaya Cave (FSC RPRV–SukC–33-43, /34-44, /35-45, /37-47). Unscaled. Blue and grey patterns as in Figure 2.

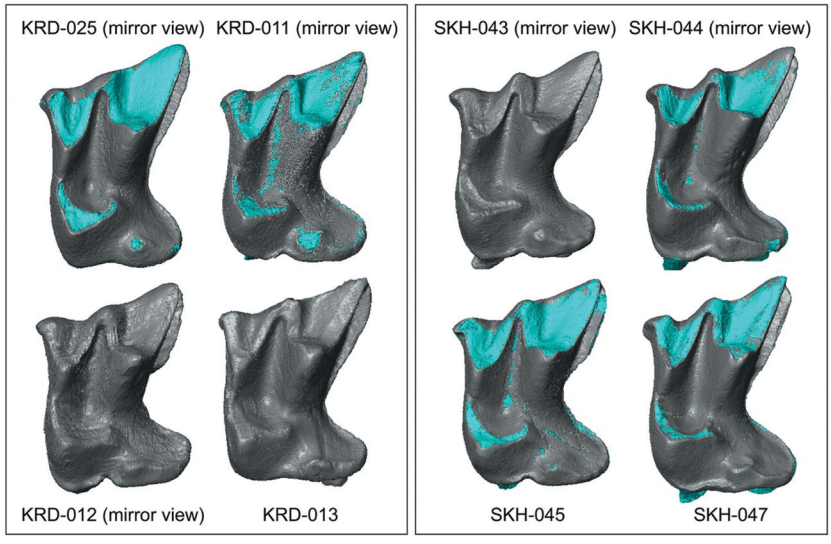

**Table C.** Recent and fossil specimen dimensions.

| Collection number | Species (age, sex) | Locality | Abbr.* | AW, mm |
|---|---|---|---|---|
| ZIN 76015 | *Crocidura lasiura* (m,s) | GVR | – | 2.26 |
| ZIN 76017 | *C. lasiura* (m,s) | GVR | – | 2.33 |
| ZIN 76019 | *C. lasiura* (f,s) | GVR | – | 2.07 |
| ZIN 76020 | *C. lasiura* (f,s) | GVR | – | 2.26 |
| ZIN 76021 | *C. lasiura* (f,s) | GVR | – | 2.23 |
| ZIN 89357 | *C. lasiura* (m,s) | KHS | – | 2.10 |
| FSC RPRV-KorC-110-11 | *C. lasiura* (?,ad) | KRD | KRD-011 | 2.38 |
| FSC RPRV-KorC-112-13 | *C. lasiura* (?,ad) | KRD | KRD-013 | 2.15 |
| FSC RPRV-SukC-33-43 | *C. lasiura* (?,ad) | SKH | SKH-043 | 2.33 |
| FSC RPRV-SukC-34-44 | *C. lasiura* (?,s) | SKH | SKH-044 | 2.35 |
| FSC RPRV-SukC-35-45 | *C. lasiura* (?,s) | SKH | SKH-045 | 2.22 |
| FSK RPRV-SukC–37-47 | *C. lasiura* (?,ad) | SKH | SKH-047 | 2.38 |
| FSC RPRV-KorC-111-12 | *Crocidura* cf. *C. lasiura* (?,ad) | KRD | KRD-012 | 2.50 |
| FSC RPRV-KorC-124-25 | *Crocidura* cf. *C. lasiura* (?,ad) | KRD | KRD-025 | 2.18 |